RSC Advances

ROYAL SOCIETY OF CHEMISTRY

www.rsc.org/advances

Effect of heat treatment of magnesium alloy substrates on corrosion resistance of a hybrid organic-inorganic sol-gel films

L. Diaz,[ab] F.R. García-Galván,[a] I. Llorente,[a] A. Jiménez-Morales,[c] J.C. Galván,*[a] and S. Feliu Jr *[a]

[a]Centro Nacional de Investigaciones Metalúrgicas (CENIM), CSIC, Avda. Gregorio del Amo 8, 28040 Madrid, Spain. E-mail: jcgalvan@cenim.csic.es; sfeliu@cenim.csic.es; Fax. +34 915347425; Tel.: +34 915538900

[b]Universidad Simon Bolivar, Departamento de Ciencias de los Materiales, Baruta, Apartado 89000, Caracas 1080-A, Venezuela

[c]Universidad Carlos III de Madrid, Departamento de Ciencia e Ingeniería de Materiales e Ingeniería Química, Escuela Politécnica Superior, Avda. de la Universidad, 30. 28911 Leganés (Madrid), Spain.

Abstract: The influence of heat treatment of magnesium alloy substrates on corrosion resistance of a sol-gel coating has been assessed during immersion tests in 0.6M NaCl aqueous solution. Relative differences in the chemical nature of the layers were quantified by scanning electron microscopy (SEM) and energy dispersive analysis of X-ray (EDX). Corrosion behaviour was evaluated by Electrochemical Impedance Spectroscopy (EIS) and hydrogen evolution measurement. Long-term immersion testing show that the sol-gel/heat treated AZ61 substrate exhibits a superior anti-corrosion property in comparison with the sol-gel/non-heated substrate. In contrast, no significant changes have been observed between the heated and non-heated samples in the case of the sol-gel coated AZ31 substrates. A link was found between lower O/Si atomic ratios observed by EDX analysis on the sol-gel coatings after the preparation process and reduced corrosion upon the coated substrates. Heat-treatment increased the protective properties of the passive film on the surface of the AZ61 substrate and hence inhibited magnesium dissolution and hydrophilic groups formation during coating preparation.

Introduction

Magnesium alloys have some advantageous properties as high dimensional stability, low density, high strength, high thermal conductivity, good damping capacity, castability and machinability and they are easily recycled.[1] These alloys show a surface film composed of MgO and $Mg(OH)_2$ which provides corrosion protection in air, but become unstable in aqueous environments.[2] One of the most effective ways to prevent corrosion of metals, is to separate the metallic surface from the corrosive medium by deposition of coating films on the surface.[3] In this case, the coatings protect the substrate by acting as a physical barrier between the metal and its environment.[4-8] Many routes may be followed for the deposition of coatings on metal surfaces, for example, electrochemical deposition, plasma spraying, physical vapour deposition, chemical vapour deposition, and sol-gel technology.[9]

The sol-gel method enables the obtaining of organic-inorganic hybrid coatings by using chemical precursors of high reactivity and purity, avoidance of corrosive by-products, improved control of the product structure, and provides an easy, cost-effective and excellent way to incorporate inorganic compounds into an organic one.[10] The organopolysiloxane coatings prepared by sol-gel process are of great interest because they combine characteristics of both organics and inorganics.[10] Such coatings display good method for the corrosion protection of metal surfaces including magnesium ones.[11-13]

The main challenges of the sol-gel process as a single technique in anti-corrosion of magnesium alloys are the high chemical activities of the substrates, and most of sols possess a low pH and contain some corrosive ions such as Cl^- or Ac^-, leading to corrosion at the beginning of coating preparation.[14] Moreover magnesium substrate in aqueous media displays a high reactivity when the sol contains a large portion of water, complicating the preparation of homogeneous coatings without pores and defects.[15]

Zhao *et al.* reported that the appropriate pH of 45S5 bioglass–ceramic coatings on AZ31 magnesium is approximately 5, because weak acidity is beneficial to the stability and uniform of gel.[16] However, hydrogen ions in gel are too aggressive for the unprotected Mg surface, and can react with magnesium. Clearly, hydrogen, in the form of bubbles, will be generated on the surface and will damage the structure of gel coating, which is considered the leading cause of cracking of the coatings on unpretreated substrates.[17] On the other hand, some authors combine sol-gel method with other surface treatments to improve the corrosion resistance of magnesium alloy.[14] Substrate pre-treatment is quite crucial in the formation of an efficient protective coating.[17] Several surface treatments prior to applying sol-gel on the magnesium alloy, including conversion coatings[18] or micro-arc oxidation[19] have been developed. These methods, however, are often rather sophisticated and may include the release of harmful substances. Heat treatments offer a simple, comparatively low-cost, and easily implemented method for improving corrosion resistance of the magnesium alloys, by altering the microstructure and/or the surface condition of the alloy without adding undesired substances.[20]

In a previous study, it was observed that the chemical composition of the thin oxide surface films induced by heating in air at 200ºC for 60 min on the freshly polished commercial AZ31 and AZ61 alloys may affect the corrosion behaviour of magnesium alloys.[21] This thermal treatment resulted in the increase of the corrosion resistance of the AZ61 alloy by approximately two or three times in the immersion test in 0.6 M NaCl solution. Following the idea that the initial external oxide film present on the Mg-Al alloys substrates may provide resistance to the initiation and propagation of magnesium corrosion, in the present research it is studied the possibility of increasing the barrier properties of silane films and improving their corrosion performance by a simply heat treatment of the metallic substrates in air at 200ºC. The objectives of the

study are as follows: (i) to study the possible changes on the sol-gel coating formed on the AZ31 and AZ61 alloys induced by the changes on the protective properties of the oxide film that forms on the surface of magnesium alloys with the heat treatment. The chemistry and morphology of the sol-gel coating grown on non-heated and heat treated AZ31 and AZ61 substrates are compared by AFM and scanning electron microscopy (SEM) and energy dispersive analysis of X-ray (EDX); (ii) to contribute to a better understanding of the influence of the composition of the sol-gel coatings formed on the surface of magnesium alloy substrates and their corrosion resistance in NaCl 0.6M solution by applying EIS and hydrogen evolution measurement.

Experimental

Samples of wrought magnesium aluminium alloy (AZ31 or AZ61) in plates of 3 mm thickness were supplied by Magnesium Elektron Ltd, Manchester, UK. The chemical compositions of the tested magnesium alloys, AZ31 and AZ61, are listed in Table 1. Freshly polished samples were dry ground through successive grades of silicon carbide abrasive papers from P600 to P2000 followed by finishing with 3 and 1 μm diamond paste, rinsed in water and dried with hot air. Due to the high affinity of magnesium to the ambient atmosphere, it was attempted to keep to a minimum (around 1 h) the exposure time to the atmosphere prior to the thermal treatment of the specimens or sol-gel application.

The thermal treatment was very simple, consisting of the horizontal exposure of 2 cm × 2 cm square samples of the AZ31 and AZ61 alloys in a convective stove at 200 °C in air for 60 min.

Table 1 Chemical composition of AZ31 and AZ61 alloys (wt.%).

Alloy	Al	Zn	Mn	Si	Fe	Ca	Mg
AZ31	3.1	0.73	0.25	0.02	0.005	0.0014	Bal.
AZ61	6.2	0.74	0.23	0.04	0.004	0.0013	Bal.

For preparation of sol-gel coatings [γ- methacryloyloxypropyltrimethoxysilane (MAPTMS) (98% from Aldrich), and tetramethoxysilane (TMOS) (98% from Fluka) have been used as received. Sols were prepared starting from a mixture of 4 mol of MAPTMS and 1 mol of TMOS. Ethanol and water were added with the molar ratio (TMOS + MAPTMS)/water/ethanol of 1/7/8.[17,22] The organic–inorganic hybrid coatings were deposited on the AZ31 and AZ61 by using a dip coating technique with a withdrawal speed of 9 cm/min and holding time of 60 s. The coated MAPTMS/TMOS-AZ31 alloy and MAPTMS/TMOS-AZ61 alloy systems were then placed in a furnace for 2 h at 120°C for curing.[17]

Surface images of both bare samples and sol–gel coated samples were obtained using an atomic-force microscope (AFM). All images (10 μm × 10 μm) were taken in the 5100 AFM/SPM from Agilent Technologies working in tapping mode using Si type AFM cantilevers with a normal spring constant of 40 N/m and a typical radius of 10 nm from Applied Nanostructures. Images were acquired at a resolution of 512 × 512 points and subjected to first-order flattening. After flattening, the root-mean-squared roughness (RMS roughness) of both bare and sol–gel coated surfaces have been calculated.

The coated substrates were also analysed by scanning electron microscopy (SEM) and X-ray energy dispersive spectroscopy (EDX) using a Hitachi S-4800 equipped with an Oxford EDX microanalysis system. The thickness of the sol–gel coatings was determined using cross-section SEM images.

Photoelectron spectra were recorded using a Fisons MT500 spectrometer equipped with a hemispherical electron analyser (CLAM 2) and a Mg Kα X-ray source operated at 300 W. The samples were fixed on small flat discs on a *XYZ* manipulator and placed in the analysis chamber. The residual pressure in this ion-pumped analysis chamber was maintained below 10^{-8} torr while data was being attained. The spectra were collected for 20–90 min depending on the peak intensities, at a pass energy of 20 eV, which is typical for high-resolution conditions. The intensities were estimated by calculating the area under each peak after smoothing and subtraction of the S-shaped background and fitting the experimental curve to a combination of Lorentzian and Gaussian lines of variable proportions. Although sample charging was observed, it was possible to determine accurate binding energies (BEs) by making references to the adventitious C 1s peak at 285.0 eV. The atomic ratios were calculated from the peak intensity ratios and the reported atomic sensitivity factors.[23] The measurements were performed at take-off angles of 45° with respect to the sample surface. The sample areas were 1 x 1 mm^2.

For the hydrogen evolution determinations, the corrosion of the sol-gel coated magnesium alloys was estimated by determining the volume of hydrogen evolved during solution immersion. Samples for hydrogen collection were cut into square coupons with dimensions of 2 × 2 × 0.3 cm and vertically immersed in 700 ml of quiescent 0.6 M NaCl for 14 days in a beaker open to laboratory air at 25 ± 2 °C. The entire sample surface was exposed to the electrolyte. Evolved hydrogen was collected in a burette above an inverted funnel placed centrally above sample. All these experiments were run simultaneously and each sample was subjected to essentially the same temperature and exposure history. The experimental difficulties and limitations of such test were recently documented.[24]

Electrochemical impedance measurements were also conducted in 0.6 M aqueous NaCl solution during 14 days of immersion at room temperature (25ºC). A Metrohm/Eco Chemie Autolab PGSTAT30 Potentiostat/Galvanostat Electrochemical System equipped with a frequency response analyser FRA32M module was used to carry out these measurements. The frequency ranged from 100 kHz to 1 mHz with 5 points/decade, whereas the amplitude of the sinusoidal potential signal was ±10 mV with respect to the open circuit potential. A conventional three-electrode setup was employed, using a silver-silver chloride (Ag/AgCl) in saturated KCl electrode and a graphite rod as reference and counter electrodes, respectively. The material under study was the working electrode. The exposed area of the working electrode was 3.14 cm^2. The electrochemical impedance experimental data were analysed by using a commercial software (ZView, Scribner Associates, Inc). This program enables to fit the impedance spectra to different equivalent circuits. The fitting data are quantified using the sum of square errors and chi-square of standard deviation (χ^2) via a complex non-linear least square method.[25] The criteria used in estimating the quality of fitting of the impedance experimental data to a given equivalent circuit were firstly the lower chi-square value and secondly by limiting the relative error in the value of each element in the equivalent circuit.

Results

Effect of substrate heat treatment on surface morphology and composition of the sol-gel coating formed on the surface of the heated AZ31 and AZ61 substrates

Figs. 1(a-d) compare the surface morphologies of the sol-gel coating grown on non-heated and heat treated AZ31 and AZ61 substrates. The surface morphology of all the sol-gel coatings looks smooth, crack-free, dense, and homogeneous. However, the non-heated AZ31 substrate reveals a less homogeneous morphology with the presence of a number of protuberances (arrows marked in Fig. 1a). In EDX analyses obtained on the spots (not shown), the increase in the Si content and the decrease in the Mg content compared to the darker regions, evidenced accumulation of silica.

Fig. 2 compares the variation in the O/Si atomic ratio of the darker regions obtained by EDX on the surface of the coated samples. The O/Si ratio is about 2.7-2.8 for the non-heated AZ31 and AZ61 substrates and heated AZ31 substrate, which is higher than the 1.9 value in the heated AZ61 substrate.

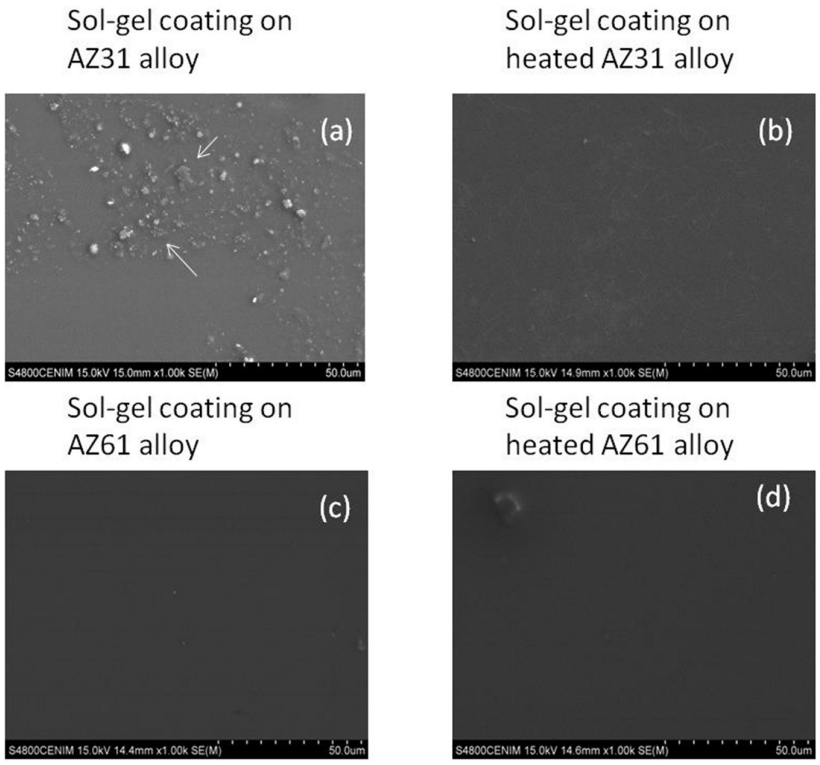

Fig. 1 SEM surface morphologies for sol-gel coating on AZ31 (a, b) and AZ61 magnesium (c,d) non-heated (a and c) and heated for 60 min (b and d) at 200 °C in air, respectively.

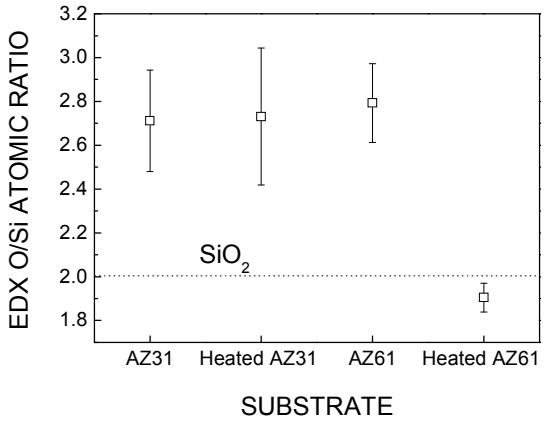

Fig. 2 Variation in the O/Si atomic ratio of the dark layer calculated from EDX analyses of the surface of the samples.

Fig. 3 compares the variation in the Al/(Al+Mg) atomic ratio of the darker regions obtained by EDX on the surface of the coated samples. No significant differences in these ratios were observed in the heated AZ31 substrate compared with the non-heated AZ31 substrate (Fig. 3). In contrast with the AZ31 sample, the Al/(Mg+Al) ratio determined by EDX is about 0.11 for the heated AZ61 substrate, which is about two times higher than the 0.06 value in the bulk alloys (Table 1) or the non-heated AZ61 substrate (Fig. 3).

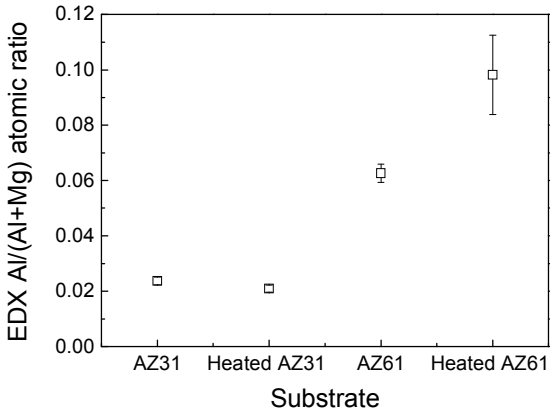

Fig. 3 Variation in the Al/(Al + Mg) atomic ratio of the dark layer obtained by EDX on the surface of the samples.

Cross-section SEM image revealed that the sol-gel coatings are continuous, crack-free and strongly adhered to the Mg-Al alloy substrates (Fig. 4a). These analyses showed that the thickness of the obtained sol-gel coatings depends of the type of the Mg-Al alloy where they were deposited. The thickness of coatings was about 2.20 µm when they were deposited on AZ31 alloy substrates[17] and 1 µm when they were deposited on the AZ61 alloy substrates (Fig. 4a). EDX analyses were used to delimit which areas of the SEM picture corresponded to the thin film of sol-gel. As an example Fig. 4b show that the EDX spectra of the image zone attributed to the coating presents higher content in O and Si than those zones which correspond to the Mg-Al alloy substrate. The increment in O and Si due to organic-inorganic nature reveals the presence of the sol-gel coating.

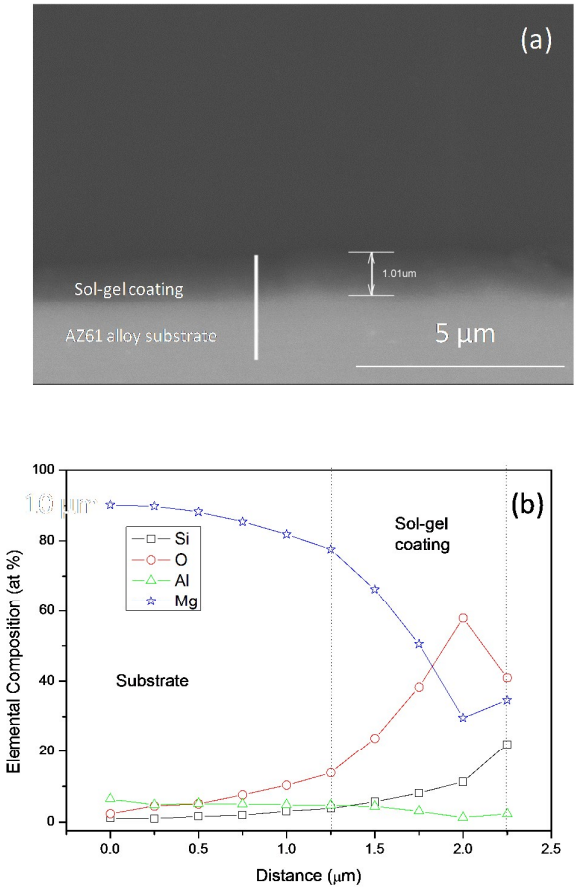

Fig. 4 SEM morphology and EDX quantitative analysis for the cross-section of the coating formed on AZ61 alloy.

Table 2 Atomic percentage observed by XPS of the external surface of coated samples.

Alloy	Sample	% C	%O	% Si	%O/%Si
AZ31	Sol-gel coated	41	41	18	2.2
	Heated and sol-gel coated	41	41	18	2.2
AZ61	Sol-gel coated	39	43	18	2.4
	Heated and sol-gel coated	42	40	18	2.2

Fig. 5 compares 3D AFM topography images of the AZ31 and AZ61 sol-gel coated samples. The AFM observations showed the formation of homogeneous and crack-free coatings on 3 of 4 tested samples (non-heated (Fig. 5a) and heated AZ31 substrate (Fig. 5c), and heated AZ61 substrate (Fig. 5d)). A significant number of protrusions appeared on the surface of the sol-gel coating grown on non-heated AZ61 substrate (Fig. 5b). The root mean square (RMS) roughness values of the AZ31 sol-gel coated samples were of 4-7 nm, which are similar to those obtained for the bare substrates (Table 3). In contrast, the RMS roughness was about 4.7 nm for the sol-gel coating grown on heat treated AZ61 substrate, which was much smaller than the value of 27 nm measured from the coated AZ61 substrate without heat treatment (Table 3), indicating that the surface structure of the sol-gel coating is improved by the heat treatment of the substrate.

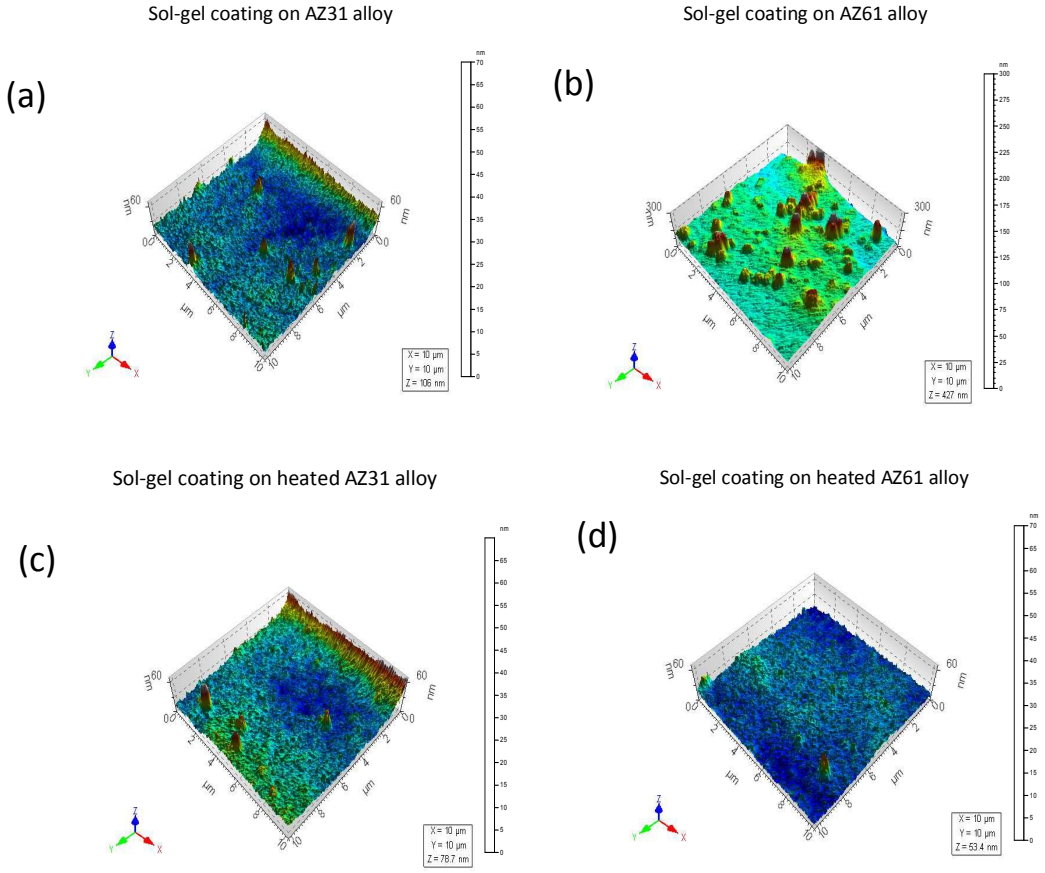

Fig. 5 AFM images of the surfaces in the sol-gel coating on AZ31 (a, c) and AZ61 magnesium (b,d) non-heated (a and b) and heated for 60 min (c and d) at 200°C in air, respectively.

Effect of substrate heat treatment on corrosion resistance of the sol-gel coating in the NaCl 0.6M solution

Electrochemical impedance measurements

Fig. 6 compares the evolution of the Nyquist plots obtained for the bare substrates with those corresponding to the sol-gel coated non-heated and heated substrates after different stages of testing. With both coated AZ31 samples, apparently one single capacitative loop at high frequencies (HF) is present during the first hour of immersion (Fig. 6a). As immersion time increased, an inductive loop at low frequencies tends to become more or less patent (Figs. 6b-6d).[27]

With the AZ61 samples, the Nyquist plots were all similar in shape (except the sol-gel coated heated substrate after 7 days of immersion) with one capacitance arc at high and medium frequencies, and an inductive loop at low frequencies (Figs. 6e-6h). For the Nyquist plots of the sol-gel coated heated AZ61 substrate after 7 days of immersion, there is only one capacitance arc (Fig. 6g).

Table 3 Roughness values obtained by atomic force microscopy

Sample	RMS roughness (nm)*
Bare substrate	
AZ31	7.4
AZ61	8.4
Sol-gel coated substrate	
AZ31	4.1
AZ61	27.1
Heated and sol-gel coated substrate	
AZ31	6.7
AZ61	4.7

* The values are average of five measurements

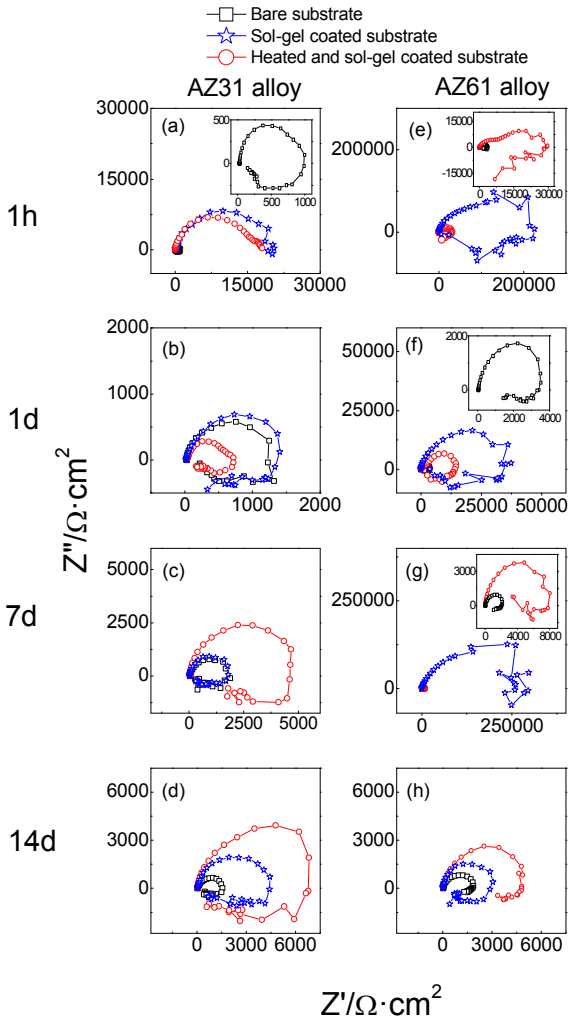

Fig. 6 Variation in Nyquist plots for AZ31 and AZ61 samples with immersion time in 0.6 M NaCl solution.

Representative impedance spectra of the tested samples in term of Bode plots are shown in Fig. 7. They seem to show the presence of two time constants which, in the Nyquist diagrams, means the presence of a capacitive loop at high frequencies and, probably, an inductive loop at low frequencies.

The impedance spectra were fitted with the equivalent circuit showed in Fig. 8 reported by King *et al.*[28] R_s represents the electrolyte resistance, C_{coat} is associated to the coating capacitance, R_{coat} is related to the pore resistance of coating. R_{corr} and C_{dl} correspond to the corrosion resistance of the metal substrate and to the double layer capacitance at the

metal/electrolyte interface respectively, both at the base of pores and damaged areas developed in the coating during immersion tests in the corrosive media (NaCl aqueous solution). Finally, L_A accounts for the variation of the extension of active anodic regions during the sinusoidal polarization and R_A represent the resistances associated to local environmental changes (precipitation of gels, presence of bubbles) nearby the anodic and cathodic regions.[29] For taking into account the intrinsic inhomogeneity of the coating and metal surface, the capacitors included in this equivalent circuit have been implemented by using Constant Phase Elements (CPEs).[30]

Mathematically, the impedance of a CPE is given by the following equation:

$$Z_{CPE} = \frac{1}{Q \cdot (j\omega)^{\alpha}} \qquad (1)$$

where j = $\sqrt{-1}$, ω is the angular frequency in rad/s, ω = 2πf, and f is the frequency in Hz. The CPE is defined by two parameters Q and α, where Q has units of s^{α}/Ω or $Fs^{\alpha-1}$ and α is a dimensionless number.[30] α is related to a non-uniform current distribution due to the surface roughness or other distributed properties, and varies between 0 and 1. The CPE reduces to a resistor for α = 0, to a Warburg element representing semi-infinite length diffusion phenomena for α = 0.5 and to an ideal capacitor for α = 1.

In the case of a parallel connection of a Constant Phase Elements CPE and a resistance R, the capacitance C associated with such a CPE can be calculated, by using the relationship:[30]

$$C = (Q \cdot R^{1-\alpha)})^{1/\alpha} \qquad (2)$$

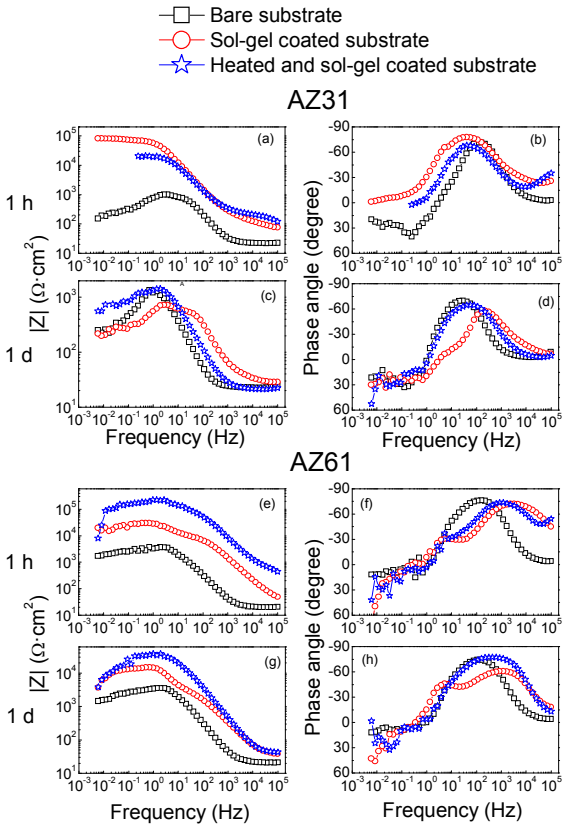

Fig. 7 Variation in Bode plots for AZ31 and AZ61 samples with immersion time in 0.6 M NaCl solution.

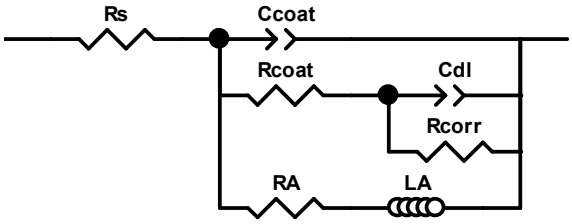

Fig. 8 Equivalent circuit used for fitting experimental EIS spectra of the samples.

Typical fitting results are compared to the experimental data in Fig. 9. Generally, the fitted and experimental impedance spectra were closely similar. Nevertheless the inductive loops observed in the experimental plots at lowest frequencies present quite noisy. The dispersion of the experimental points associated to this inductive regions usually exceed ±15% and the χ^2 are quite high. As a general rule, the fitting result was

only accepted when the fitting χ^2 parameter was ≤ 5 x 10^{-3}. Fortunately, capacitive arcs seen in these impedance plots are free of noise. Moreover the electrical elements of the equivalent circuit associated to these arcs are very representative for this type of studies. Table 4 present the numerical results of the fitting procedure.

The resistance and capacitance of the sol-gel film depend on the porosity of the coating, its crack ability, amount of absorbed water and thickness.[8,11,17]. The evolution of resistance and capacitance associate to the high frequency (HF) arc of the Nyquist plots during the immersion is presented in Figs. 10 and 11. This HF arc is related with the charge-transfer and the double layer capacitance of the bare metal substrate. For early stages of degradation of the metal/coating system this HF arc is related with the intrinsic properties of the sol-gel coating (R_{coat} and C_{coat}).[5,8] As barrier degradation of coating progresses this HF arc may depend upon the joint influence of R_{coat}/C_{coat} and R_{corr}/C_{dl}, and perhaps almost exclusively on R_{corr}/C_{dl} at the base of pores and damaged areas of sol-gel coating.[5]

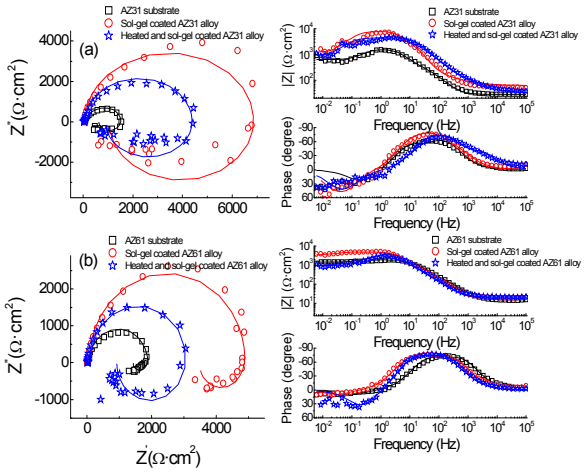

Fig. 9 Nyquist and Bode plots with respective fitting for AZ31 and AZ61 substrates, non-heated and heated sol-gel coated samples after 14 days of immersion in 0.6 M NaCl solution.

According to the literature, the pore resistance of coating, R_{coat}, which reflects the anti-penetrating ability of the coating to electrolyte through the coating pores, is an appropriate parameter to evaluate corrosion resistance of the coating.[31,32] One order of magnitude difference of initial values of R_{coat} indicates significantly lower amount of conductive pathways (pores and micro-cracks) for the sol- gel coating grown on heat treated AZ61 substrate (Fig. 10b).[11]

Table 4. Fitting parameters obtained from the capacitive arcs of Nyquist plots after 2 weeks of immersion in NaCl solution

Alloy	Sample	Equivalent circuit parameters								
		R_{coat} $(\Omega\cdot cm)^2$	$Y_{0,coat}$ $(\mu\Omega^{-1}\cdot cm^{-2}\cdot s^{-\alpha 1})$	α_1	C_{coat} $(\mu F\cdot cm^{-2})$	R_{corr} $(k\Omega\cdot cm^2)$	$Y_{0,cd}$ $(\mu\Omega^{-1}\cdot cm^{-2}\cdot s^{-\alpha 2})$	α_2	C_{dl} $(\mu F\cdot cm^{-2})$	$10^{-3}\cdot(\chi^2)$
AZ31	Sol-gel coated substrate	46.7	4.6	0.9	1.8	13.2	0.8	1.0	0.8	1.4
	Heated and sol-gel coated substrate	157	1.7	0.9	0.7	7.2	1.3	0.9	0.8	1.8
AZ61	Sol-gel coated substrate	16.2	1.6	1.0	1.6	10.2	10.2	0.8	5.8	0.9
	Heated and sol-gel coated substrate	46.9	7.8	0.9	3.2	6.8	1.7	1.0	1.7	0.6

After 1 day of immersion, the R_{coat} values for the sol-gel coated AZ31 samples and sol-gel coated AZ61 sample show a remarkable reduction, nearly close to the values of the bare substrate, which may be attributed to, the absorption of liquid into the sol-gel and the attack of corrosive species, and maintained these values up to 14 days of immersion (Fig. 10). This suggests that the sol-gel coating, in some way, does not act as an effective barrier to prevent the penetration of the electrolyte. In spite of the fall in the initial values of the R_{coat} value of the coated heated AZ61 sample after 1day of immersion that occurs due to the electrolyte uptake, it remains at least three times higher when

compared to other coated samples and the bare substrate (Fig. 10b) confirming superior stability and barrier properties of the coating to corrosive solution. After 7 days of immersion, a significant recovery of R_{coat} values for the coated heated AZ61 substrate is observed, which can be ascribed to the precipitation of corrosion products, which block the pores/defects at the sol-gel films. At the end of 14 days of immersion, the value of R_{coat} of the coated heated AZ61 substrate was in the same order of magnitude than the other samples studied (Fig. 10b).

The rate of water uptake and the hydrolytic stability of coatings during immersion in aqueous solutions can be determined from the evolution of the capacitance of the sol-gel film.[33] The evolution of coating capacitance for the different samples in 0.6M NaCl aqueous solution is presented in Fig. 11. It can be seen that the capacitance values associated with the coated AZ61 samples at the initial immersion time are one order magnitude smaller compared to bare substrate or coated AZ31 samples emphasizing the initial barrier properties of the sol-gel coating.

The evolution of the values of C_{coat}, which gradually increases after immersion, corroborates the conclusions obtained from the R_{coat} parameter. These behaviors are attributed to the uptake of the chloride and water through pores and cracks of the silica network leading to filling of pores and increasing of the amount of absorbed water.[34]

It can be found in Fig. 11 that the C_{coat} of the coated heated AZ61 substrate keeps a stable value of around 0.7 F $\mu F/cm^2$ in 7 days immersion time. This means that the sol-gel coating can be a barrier for electrolyte for a long period of time. Compared with that of other sol-gel coated samples, the decrease rate is markedly slower which may be related with an increase of the barrier properties and stability of the sol-gel coating grown on the heated AZ61 substrate.[11] After 14 days, the capacitance values for all the tested samples are grouped around 3-10 $\mu F/cm^2$ (Fig. 11).

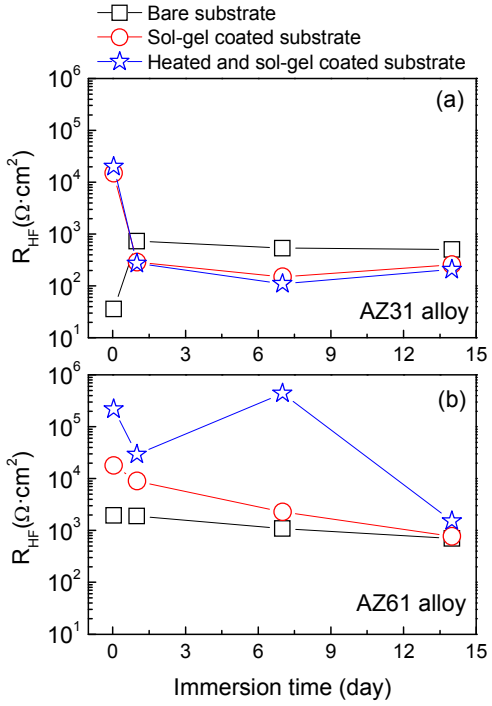

Fig. 10 Evolution of the resistance (R_{HF}) associated to the high frequency arc with immersion time in NaCl 0.6M solution.

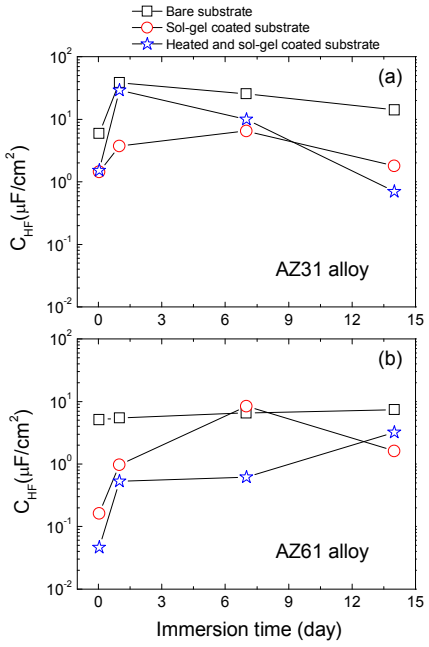

Fig. 11 Evolution of the coating capacitance (C_{HF}) associated to the high frequency with immersion time in 0.6M NaCl aqueous solution.

Hydrogen evolution measurements

Fig. 12 compares the hydrogen evolution versus time curves (direct measure of the corrosion rate) for the bare AZ31 alloy and sol-gel coated substrates (a) and those corresponding to the AZ61 alloy (b) during immersion in 0.6 M NaCl for 14 days. No significant differences were observed in these curves for the two sol-gel coated AZ31 samples compared to the bare alloy. From Fig. 12a it can be deduced that the hydrogen evolution data for the AZ31 alloy progresses according to an approximately parabolic law typical of a process that is under control by diffusion, possibly associated with the effect of the precipitation of insoluble and protective magnesium corrosion products on the sol-gel coating.[17]

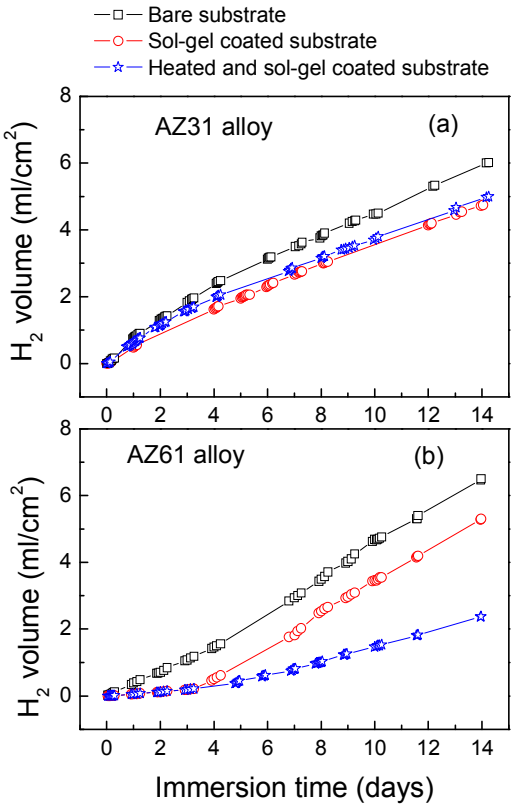

Fig. 12 Variation in H_2 evolution volume values for the samples over 14 days immersion in 0.6 M NaCl aqueous solution.

Two different regimes were observed in the corrosion rate curve of the coated AZ61 alloy substrates: an initial period of relatively small evolved hydrogen volume and, after about 3 to 5 days, a much less protective effect with a moderately accelerated linear kinetics attributed to the breakdown of the sol-gel film and activation of microgalvanic acceleration of the corrosion by the significant β phase fraction in the AZ61 alloy.[17] There was a significant difference in the rate of hydrogen evolution for the three samples, with heated and sol-gel coated AZ61 substrate having the lowest hydrogen evolution rate (Fig. 12b), i.e. better corrosion resistance, which is in accordance with the result of EIS measurements.

Fig. 13 compares photographic images of the samples taken throughout the hydrogen evolution test. After immersion in 0.6M NaCl solution copious amounts of gas bubbles resulting from the dissolution of coated and bare AZ31 samples were generated and accumulated on their surface. After 1 day, in addition to the large amounts of bubbles, these samples present much of its surface covered by dark corroded areas (Fig. 13). According to a previous study,[35] filiform corrosion was initiated almost immediately on the AZ31 sample after immersion, and the population of filaments expanded in less than one day across the entire exposed surface. The appearance of dark corrosion areas (Fig. 13) is consistent with the fast decrease of the initial values of the impedance for the coated AZ31 samples (Figs 6a and 6b and 7a and 7b). After 5 days of immersion, white corrosion products appeared on the surface of the AZ31 samples. In contrast, there were no significant bubbles accumulated on the AZ61 samples and their surface is much lighter in color than the AZ31 samples held under the same immersion conditions (Fig. 13) that can be treated as an indication of the marked attenuation in the corrosion process.

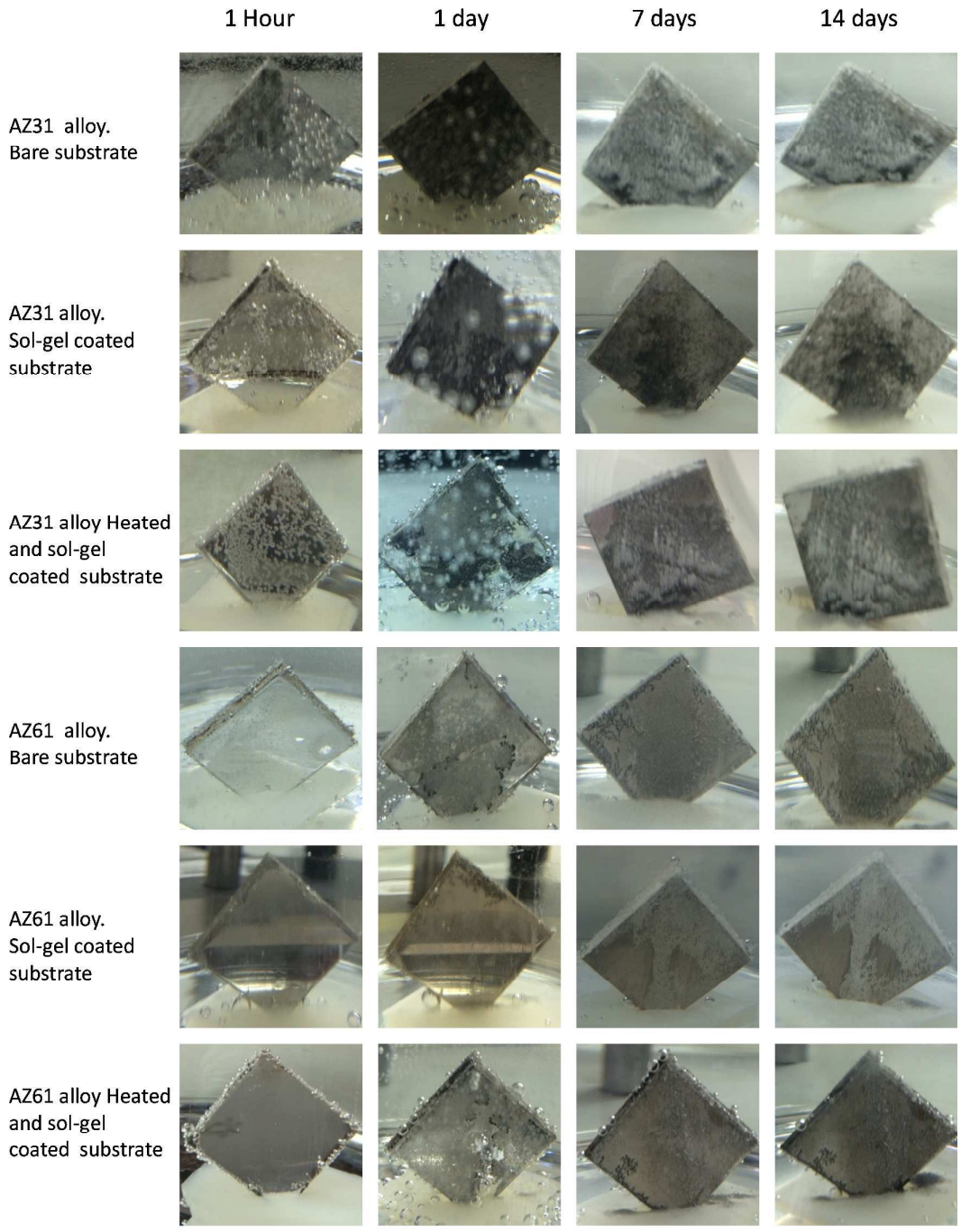

Fig. 13 Photographic images of the evolution of corrosion morphology with immersion time for the samples used in the H_2 evolution test.

Discussion

Influence of the heat treatment of Mg-Al alloys substrate on the sol-gel coatings formed

The EDX (Fig. 3) analyses suggest a considerable superficial aluminium species enrichment of the AZ61 substrate that had been heat treated. Growth of the oxide film requires the motion of reactants for some transport mechanism. In Mg–Al Alloys, diffusion rates of Mg and Al ions may influence their concentration in the oxide film formed on the alloy surface. Recent data in the literature,[36,37] suggest that in the MgO (periclase) trivalent cations diffuse rapidly compared to divalent cations, behaviour arising from the coulombic attraction between trivalent cations and cation vacancies; for this reason diffusion of Al^{3+} can be one order of magnitude faster than Mg^{2+} at the same conditions. This could favour the increases in Al concentration highlighted in the paper.

Also, the EDX (Fig. 2) analyses reveals that sol-gel coating grown in the heat treated AZ61 substrate has a ratio of O/Si equal to 1.9 which is very close to 2.0 value corresponding to the O/Si ratio from SiO_2 oxide. Liang *et al*. observed Si:O molar ratio of 11.68:26.51 in the EDX analysis of an aluminum substrate covered with a tetraethtylorthosilicate (TEOS) film, which was estimated as a result from the formation of SiO_2 nanoparticles when film was hydrolyzed and condensed.[38] The O/Si ratio for the other three coated samples showed an increased oxygen concentration with O/Si ratio to be 2.7-2.8. Silane-based sol–gel coatings are known for their low hydrolytic stability in alkaline medium.[39] Magnesium surface always has high alkalinity in an aqueous solution because of its reaction with water:

$$Mg + 2H_2O \rightarrow Mg^{2+} + 2OH^- + H_2\uparrow \qquad (3)$$

This is a rapid alkalization reaction.[40] The local pH of cathodic reactions rising to a value of 10 could accelerate the hydrolytic decomposition of the of the SiO_2 network.[39,41] The higher O/Si atomic ratio found in the sol-gel coating formed on the non-heated AZ31

and AZ61 and heat treated AZ31 substrates compared with the heated AZ61 substrate is consistent with a significant magnesium dissolution and pH of the liquid adjacent to the metallic surface increase during the polymer deposition reaction with the preferential formation of hydroxyl containing type compounds.

By using the same heat treatments and alloys, Feliu *et al*. observed a strong link between the degree of metallic Al enrichment in the subsurface layer (from 10 to 15 at.%) observed by X-ray photoelectron spectroscopy (XPS) in the AZ61 heat treated samples.[21] With the help of electrochemical impedance spectroscopy (EIS) they also observed an increase in protective properties of these systems when they are submitted to immersion test in 0.6 M NaCl.[21] At the beginning of the sol-gel coating formation, it is likely that this protective and homogeneous surface layer initially present on the heat treated AZ61 substrate had a greater capability to isolate this alloy from the aqueous electrolyte environment and the effects of magnesium dissolution compared to the other samples with the result of the growth of a more perfect sol-gel coating.

Relationship between the composition of the sol-gel coatings and their corrosion resistance in saline solutions

It seems likely that some differences revealed in the composition characteristics of sol-gel films formed on alloy AZ31 and AZ61 substrates after the heat treatment may have an impact on the corrosion behaviour of the samples in saline solutions.

The heat treatment of the AZ61 substrates strongly improves the barrier properties of the coating. The EIS results show that the coating resistance for coated heated AZ61 substrate increases by at least one order of magnitude comparatively to the other coated samples during the first 7 days of exposure (Fig. 10). Apart from the increase R_{coat}, the decrease in C_{coat} values (Fig. 11) is also a piece of evidence for the hydrophobic effect of the surface, which could effectively decrease the direct contact of

the substrate to corrosive medium and thus improve the long-term corrosion resistance.[41] Li *et al*. observed that the sol-gel film formed on aluminium was more protective in sodium chloride solutions than that on copper.[42] According to these authors the Al metal is better passivated than Cu under ambient condition and the passive layer would help to develop a rather high barrier of intermediate layer for corrosion protection in the sol–gel-coated sample.[43] In this study, the heat treatment of the AZ61 substrate presumably inhibits the magnesium dissolution during the preparation process decreasing the concentration of hydrophillic surface hydroxyls groups on the sol-gel coating surface, as confirmed by the lower O/Si atomic ratio observed by EDX (Fig. 2), improving substantially the surface hydrophobicity and barrier properties of the films.[43]

In contrast to the findings with the heated AZ61 substrate, the EIS data for the coated and non-heated AZ31 and AZ61 substrates and heat treated AZ31 substrate commented above indicate that the sol-gel coating does not prevent significantly the corrosion (Figs. 10 and 11). In these substrates, it is probable that the enrichment in hydroxyl groups resulting from the preparation process enhances the hydrophilic nature of the silica matrix decreasing drastically the barrier properties of the coating. The hydrophilic characteristics of the sol-gel coating formed on these substrates may be consistent with the higher O/Si atomic ratio observed by EDX (Fig. 2).

Conclusions

AFM and SEM/EDX analyses revealed that the sol-gel coatings formed on the surface of AZ61 substrate as a result of heating at a temperature of 200ºC for 1 hour are far the more perfect, uniform and free of nanoscopic defects, and presenting lower EDX O/Si atomic ratios than those formed on the non-heated AZ61 substrate. Curiously, this phenomenon has not been detected in the AZ31 alloy subjected to identical treatment.

Attention is drawn to the aluminium enrichment on the surface layer of the AZ61 substrate owing to the heat treatment.

The native oxide film formed on the surface of AZ61 substrates during thermal treatment seems to be sufficiently protective to prevent some magnesium dissolution and the associated hydrogen evolution during the curing process of the sol-gel film formation.

Coating resistance values calculated from EIS measurements in an interval between 1 h and 14 days of immersion in 0.6M NaCl solution, have allowed the establishment of relationships between the properties of the sol-gel coating formed on the different substrates and their corrosion resistance. Probably due to the effect of a defective coating, in the first hour of immersion in 0.6M NaCl coating resistance values for the non-heated AZ61 substrates are about ten times lower than the values corresponding to the heated substrate attributed to a more protective barrier effect of the sol-gel film formed. This effect is not shown in the AZ31 substrate, and suggests the existence of a strong link between O/Si atomic ratios observed by EDX analysis on the sol-gel and corrosion resistance of the coated surfaces.

With regard to the protective properties of the sol-gel film formed, after seven days of immersion the coating resistance values for the heated AZ61 substrate significantly exceed that of the non-heated substrate. Only after 15 days of testing the differences between the impedance diagrams of heated AZ61 substrates and the corresponding non-heated ones tends to disappear.

Acknowledgements

The authors express their gratitude to Prof. S. Feliu for several clarifying and stimulating discussions during the course of this work. They also gratefully acknowledge financial

support for this work from the Ministry of Economy and Competitiveness of Spain (MAT2009-13530 and MAT2012-30854).

References

1 J. Zhang, Z. Zhang, Magnesium alloys and their applications, *Chemical Industry Press of China*, Beijing, 2004.

2 T.T. Hu, B. Xiang, S.G. Liao, W.Z. Huang, *Anti-Corros. Methods Mater.*, 2010, 57, 244.

3 H. Altun, H. Sinici, Mater. Charact., 2008, 59, 266-270.

4 H. Leidheiser Jr., *Corrosion*, 1982, 38, 374.

5 S. Feliu, J.C. Galván, M. Morcillo, *Prog. Org. Coat*., 1989, 17 (2), 143.

6 G. Grundmeier, W. Schmidt, M. Stratmann, *Electrochim. Acta*, 2000, 45 (15-16), 2515.

7 V. Barranco, S. Feliu Jr., S. Feliu, *Corros. Sci*., 2004, 4, 2221.

8 M. García-Heras, A. Jiménez-Morales, B. Casal, J.C. Galván, S. Radzki, M.A. Villegas, *J. Alloys Compd.*, 2004, 380, 219-224.

9 C.J. Brinker, A.J. Hurd, P.R. Schunk, G.C. Frye, C.S. Ashley, *J. Non-Cryst. Solids*, 1992, 147, 424.

10 A.A. El Hadad, D. Carbonell, V. Barranco, A. Jiménez-Morales, B. Casal, J.C. Galván, *Colloid Polym. Sci.*, 2011, 289, 1875.

11 S.V. Lamaka, M.F. Montemor, A.F. Galio, M.L. Zheludkevich, C. Trindade, L.F. Dick, M.G.S. Ferreira, *Electrochim. Acta*, 2008, 53 (14), 4773.

12 V. Barranco, N. Carmona, J.C. Galván, M. Grobelny, L. Kwiatowski, Prog. Org. Coat., 2010, 68, 347.

13 R.G. Hu, S. Zhang, Su; J.F. Bu, C.J. Lin, G.L. Song, *Prog. Org. Coat.*, 2012, 73 (2-3), 129.

14 X.K. Zhong, Q. Li, B. Chen, J.P. Wang, J.Y. Hu, W.Hu, *Corros. Sci.*, 2009, 51 (12), 2950.

15 N.V. Murillo-Gutiérrez, F. Ansart, J-P. Bonino, S.R. Kunst, C.F. Malfatti, *Appl. Surf. Sci.*, 2014, 309, 62.

16 H. Zhao, S. Cai, S.X. Niu, R.Y. Zhang, X.D. Wu, G.H. Xu, Z.T. Ding, *Ceram. Int.*, 2015, 41 (3) 4590, Part B.

17 A.A. El-Hadad, V. Barranco, A. Samaniego, I. Llorente, F.R. García-Galván, A. Jiménez-Morales, J.C. Galván, S. Feliu, *Prog. Org. Coat*., 2014, 77 (11) 1642.

18 N.V. Murillo-Gutiérrez, F. Ansart, J-P. Bonino, M-J. Menu, M. Gressier, *Surf. Coat. Technol*., 2013, 232, 606.

19 C.J. Wang, B.L. Jiang, M. Liu, Y.F. Ge, *J. Alloys Compd*., 2015, 621, 53.

20 A.C. Hänzi, P. Gunde, M. Schinhammer, P.J. Uggowitzer, *Acta Biomater*., 2009, 5 (1), 162-171.

21 S. Feliu Jr., A. Samaniego, V. Barranco, A.A. El-Hadad, I. Llorente, C. Serra, J.C. Galván, *Appl. Surf. Sci.*, 2014, 295, 15, 219.

22 A. Jiménez-Morales, J.C. Galvan, P. Aranda, E. Ruiz-Hitzky, *Mater. Res. Soc. Symp. Proc*., 1998, 519, 211.

23 C.D. Wagner, L.E. Davis, M. V. Zeller, J.A. Taylor, R.H. Raymond, L.H. Gale, *Surf. Interface Anal.*, 1981, 3, 211-225.

24 N.T. Kirkland, N. Birbilis, M.P. Staiger, *Acta Biomater.*, 2012, 8, 925.

25 ZView software, Version 3.4d (Scribner Associates Inc), Southern Pines, NC, USA.

26 Y. Tamar, D. Mandler, *Electrochim. Acta*, 2008, 53 (16), 5118-5127.

27 S. Feliu, C. Maffiotte, J.C. Galván, V. Barranco, *Corros. Sci.*, 2011, 53 (5), 1865.

28 A.D. King, N. Birbilis, J.R. Scully, Electrochim. Acta, 2014, 121, 394.

29 M. Curioni, F. Scenini, T. Monetta, F. Bellucci, *Electrochim. Acta*, Volume 2015, 166, 372.

30 M.E. Orazem, I. Frateur, B. Tribollet, V. Vivier, S. Marcelin, N. Pebere, A.L. Bunge, E.A. White, D.P. Riemer, *J. Electrochem. Soc.*, 2013, 160 (6), C215.

31 X.W. Liu, J.P. Xiong, Y.W. Lv, Y. Zuo, *Prog. Org. Coat*., 2009, 64, 497.

32 S.V. Lamaka, H.B. Xue, N.N.A.H. Meis, A.C.C. Esteves, M.G.S. Ferreira, *Prog. Org. Coat.*, 2015, 80, 98.

33 M.L. Zheludkevich, R. Serra, M.F. Montemor, K.A. Yasakau, I.M. Miranda Salvado, M.G.S. Ferreira, *Electrochim. Acta*, 2005, 51 (2), p. 208.

34 V. Dalmoro, J.H.Z. dos Santos, C. Alemán, D.S. Azambuja, Corros. Sci., 2015, 92, 200.

35 A. Samaniego, I. Llorente, S. Feliu Jr., *Corros. Sci.*, 2013, 68, 66-71.

36 J.A. Van Orman, K.L. Crispin, *Rev. Mineral. Geochem*., 2010, 72, 757.

37 B.H. Zhang, X.P. Wu, *Chin. Phys. B* 22 (2013) 056601.

38 Jin Liang, Yunchu Hu, Yiqiang Wu, Hong Chen, *Surf. Coat. Technol.*, 2014, 240, 145.

39 V. Lamaka, G. Knörnschild, D.V. Snihirova, M.G. Taryba, M.L. Zheludkevich, M.G.S. Ferreira, *Electrochim. Acta*, 2009, 55 (1), 131.

40 G.L. Song, *Electrochim. Acta*, 2010, 55 (7), 2258-2268

41 A. Zomorodian, F. Brusciotti, A. Fernandes, M.J. Carmezim, T. Moura e Silva, J.C.S. Fernandes, M.F. Montemor, *Surf. Coat. Technol*., 2012, 206, 21, 4368.

42 Y.S. Li, A. Ba, M.S. Mahmood, *Electrochim. Acta*, 2008, 53 (27), 7859.

43 V. Dalmoro, J.H.Z. dos Santos, L.M. Baibich, I.S. Butler, E. Armelin, C. Alemán, D.S. Azambuja, *Prog. Org. Coat*., 2015, 80, 49.

GRAPHICAL ABSTRACT

Sol-gel coating on AZ31 alloy

(a)

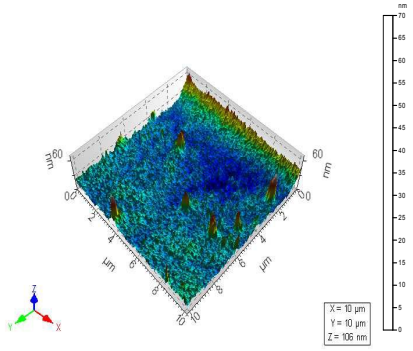

Sol-gel coating on AZ61 alloy

(b)

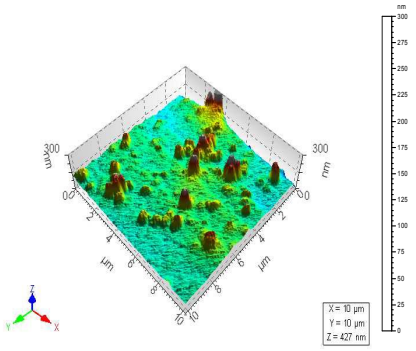

Sol-gel coating on heated AZ31 alloy

(c)

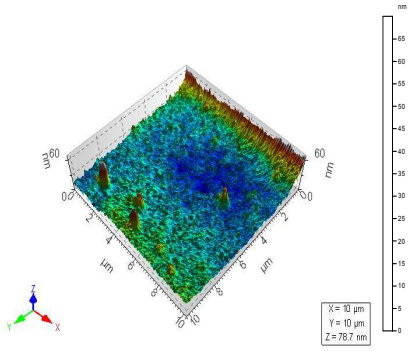

Sol-gel coating on heated AZ61 alloy

(d)